Journal of Materials Chemistry A

Anti-frost coatings containing carbon nanotube composite with reliable thermal cyclic property

Journal:	*Journal of Materials Chemistry A*
Manuscript ID:	TA-ART-03-2014-001398.R1
Article Type:	Paper
Date Submitted by the Author:	11-May-2014

Complete List of Authors:	Sohn, Yoonchul; Samsung Advanced Institute of Technology, Kim, Dongouk; Samsung Advanced Institute of Technology, Lee, Sangeui; Samsung Advanced Institute of Technology, Yin, Mingming; Samsung Electronics, Song, Jae Yong; Korea Research Institute of Standards and Science, Hwang, Wootaek; Samsung Electronics, Park, Sung-Hoon; Samsung Advanced Institute of Technology, Kim, Hajin; Samsung Advanced Institute of Technology, Ko, Youngchul; Samsung Electronics, Han, Intaek; Samsung Advanced Institute of Technology,

Journal Name

RSCPublishing

ARTICLE

Anti-frost coatings containing carbon nanotube composite with reliable thermal cyclic property

Cite this: DOI: 10.1039/x0xx00000x

Yoonchul Sohn,[a] Dongouk Kim, [a] Sangeui Lee, [a] Mingming Yin, [b] Jae Yong Song, [c] Wootaek Hwang, [b] Sunghoon Park, [a] Hajin Kim, [a] Youngchul Ko [b] and Intaek Han *[a],

Received 00th January 2012,
Accepted 00th January 2012

DOI: 10.1039/x0xx00000x

www.rsc.org/

One of the most important applications for superhydrophobic coatings is anti-frosting for safety and energy conservation. Safety concerns are especially critical in cold-climate regions where the daily temperature fluctuation is large. However, superhydrophobic coatings have not been studied in terms of their thermomechanical reliability. In this study, wetting characteristics and stress relaxation behavior were quantitatively investigated with multi-walled carbon nanotube (MWNT)–silicone composite films under thermal cycling condition. It is concluded that an open structure with numerous nanopores among the fillers, constituting air pockets described as the "Cassie structure," is of great importance not only for developing a film's superhydrophobic nature but also for accommodation of thermal stress that evolved from different coefficients of thermal expansion between the coating and the substrate. The amount of stress relaxation for a 30 vol% MWNT–silicone composite film with open structure reaches ~80% of the value for its counterpart with a closed structure and no pores. A superhydrophobic MWNT–silicone composite film that can endure over 4000 thermal cycles (-30℃ to room temperature) is fabricated by controlling the composition and microstructure of the composite. In addition, the importance of size and shape of nanofillers in delaying nucleation and growth of frost on superhydrophobic coatings is also discussed.

Introduction

Ice-repellent shields are one of the most important applications of superhydrophobic coatings. A superhydrophobic surface is known to reduce accumulation of snow, ice, or frost.[1–10] An anti-ice coating is important in terms of safety and energy conservation. Spread over a surface, even a thin layer of ice is enough to bring down power lines, burst pipes, or make roads impassable. Ice accumulation also causes dangerous loss of lifting force of aircraft wings. Accumulated ice is so sturdy that a rubber coating on airplane surfaces, designed to crack ice by inflating, cannot break thick ice. As a result, large amounts of energy are consumed to remove the frost overlayers every year.

[a] Materials Research Center, Samsung Advanced Institute of Technology, Samsung Electronics, Suwon 443-803, Republic of Korea.

[b] Eco Solution Team, Digital Media & Communications R&D Center, Samsung Electronics, Suwon 443-742, Republic of Korea.

[c] Center for Nanomaterials Characterization, Korea Research Institute of Standards and Science, Daejeon 305-340, Republic of Korea.

* intaek.han@samsung.com

Electronic Supplementary Information (ESI) available: [Calculation of thermal stress and stress relaxation of superhydrophobic MWNT–silicone composite]. See DOI: 10.1039/b000000x/

Superhydrophobic materials were first tested for anti-ice applications by Saito et al.[1] and more recently by several other groups, and they have demonstrated promising anti-icing performances.[2–10] Reduced ice adhesion was reported with the effect of wetting hysteresis on ice adhesion strength. Tourkine et al.[2] reported delayed water freezing on rough superhydrophobic surfaces, which is believed to be favorable for reduced ice accumulation, whereas Cao et al.[4] and Wang et al.[5] reported low ice accumulation on superhydrophobic surfaces exposed to natural outdoor "freezing rain" conditions. Most recently, Jung et al.[10] summarized that in addition to a hydrophobic rough surface, a smooth wettable surface with nanometer-scale roughness also showed long freezing delay. In real-life situations, superhydrophobic coatings usually undergo thermal cycling with daily movements of the sun. Despite its importance, a quantitative study on the reliability of superhydrophobic coatings under thermal cycling condition has not been published.

Carbon nanotube (CNT)-based composite materials have been investigated for various applications to improve electrical and thermal conductivities, mechanical strength, and so on. One important application is using CNT-based composite materials in superhydrophobic coatings.[11–20] Although many such applications exist, there are barely any investigations on frost formation on superhydrophobic CNT composite films. In this study, we introduce a quantitative analysis of the reliability of superhydrophobic CNT–silicone composite coatings under

thermal cycling condition. The filler (CNT) content was varied to investigate the correlation between microstructures of the composite films and their wetting characteristics. The study results show that the nanoporous structure of superhydrophobic coatings is of great importance for both wetting characteristics and the mechanical reliability to accommodate the large thermal stress imposed on superhydrophobic coatings.

Experimental

Multi-walled carbon nanotubes (MWNTs) with diameters of 10–15 nm and lengths of 10–15 μm, CM-95, were purchased from Hanwha Nanotech. The MWNTs were immersed in a solvent (chloroform) and were dispersed using ultrasonic vibration for 20 min in a tip-type machine with a power of 90 W set at a pulse ratio of 9:1 (on:off). The solution was ultrasonically agitated again for 20 min after adding a CNT dispersant, Triton X-100 surfactant (polyethylene oxide (9) nonyl phenyl ether, 5 wt% of MWNT). A silicone elastomer, Sylgard 184 from Dow Corning, was used as the polymer matrix for the composite. After adding Sylgard 184A, the ultrasonic treatment was repeated for 1 hr. Sylgard 184B was then added and the duration of the ultrasonic agitation was reduced to 10 min to minimize hardening. During the ultrasonic vibration, the solutions were immersed in a cold bath to inhibit heating. A spray coater with a nozzle diameter of 2.5 mm was used for deposition of the MWNT–silicone composites on aluminum and silicon substrates at room temperature. The spraying pressure was set at 0.68 MPa. During the coating process, the solvent was evaporated and only MWNT–silicone composite coatings remained on the substrates. To acquire good adhesion between the composites and the substrates, the Al substrates were pre-coated with X-33-173 primer (epoxy-functionalized silane coupling agents supplied by Shin-Etsu Chem. Corp.), followed by curing for 30min at 60°C. The Si substrates were pre-treated with a piranha solution (70 vol% H_2SO_4 + 30 vol% H_20_2) at 80 °C for 1 hr, followed by immersion in a 1 vol% solution of 3-glycidoxypropyltrimethoxysilane (GPTMS) for 12 h at room temperature. The MWNT content of the solvent was controlled at a level of 0.05–0.1 vol%. The MWNT content in the silicone matrix was varied from 5 to 10, 20, 30, and 40 vol% to change the resulting microstructures of the composite coatings. The prepared MWNT–silicone coatings were then heated for 1 hr at 120 °C to remove the solvent and to completely cure the silicone elastomer.

Measurements of the water contact and sliding angles were conducted to estimate the wetting characteristics of the composite coatings. Frost growth on the MWNT–silicone composite was evaluated by holding the samples inside a refrigerator at -30 °C for up to 650 min. Water molecules were continually provided in the form of moisture by keeping the door open for 15 sec every 2 hr. The relative humidity in the laboratory was controlled to remain at 40%. The microstructures of the composite coatings were observed with a scanning electron microscope (Hitachi UHR-SEM S-5500). The change in stress levels of the MWNT–silicone coatings on Si (100) substrates was measured under vacuum condition (1 x 10^{-6} Torr) by a laser wafer-curvature-measuring equipment (MOS, K-Space Associates Inc., Dexter, MI). During the measurements, the heating and cooling rates were set at 5 K/ min and the temperature range was -100 to 80 °C. The change in curvature of the backside of Si was scanned because the laser was randomly scattered on the rough surface of the composite coatings. The thickness and biaxial modulus of the Si (100) substrate used for the experiment were 675 μm and 180.5 GPa, respectively.

The reliability at low temperature was evaluated by measuring the wetting and sliding angles of the MWNT–silicone composite coatings on Al substrates after repeated thermal cycling (up to 4000 cycles). The points of measurement were selected randomly on each sample and the averaged values were obtained from five point measurements. As a result, relatively large variations were observed in some specimens. Each cycle consisted of refrigeration at -30 °C for 40 min, followed by defrosting for 20 min by powering off with the refrigerator door open (the temperature rose to 20 °C during the intermission). At the initial stage, the frost completely melted away during the intermission. However, after 2000 cycles, only the surface of the frost melted while the frost body remained frozen.

Results and discussion

First, we characterized the wetting properties of MWNT–silicone composite films as functions of MWNT content. We then investigated frost growth on the superhydrophobic coatings and estimated the critical nucleus radius for ice nucleation. The amount of thermal stresses that evolved from the difference in coefficients of thermal expansion (CTEs) of the coatings and Si substrate was calculated and compared with experimentally measured values obtained using a laser curvature-measuring equipment, from which the amount of stress relaxation could be deduced. Finally, the performance of the superhydrophobic coating with high thermal cyclic reliability was verified by conducting a thermal cycling test.

Wetting characteristics of MWNT–silicone coatings

The microstructures of MWNT–silicone films changed with varying MWNT content embedded in the composite materials. Scanning electron microscope (SEM) micrographs are presented in Figure 1. The porosity of the composite surfaces increased with increasing MWNT content, as shown in the figure. With low MWNT content (5 and 10 vol%), the MWNTs were completely embedded in the silicone matrix. On the other hand, as the MWNT content increased (20 and 30 vol%), a large number of porous spaces formed in the MWNT network inside the composite films. In this case, individual MWNTs or MWNT bundles, entangled with one another, were covered with a very thin silicone layer on their surfaces. The porous cavities inside the composite films can function as air pockets when they settle under water droplets and can therefore form the "Cassie state",[21,22] which is of great importance for developing the films' superhydrophobic nature.

Measured contact and sliding angles of MWNT–silicone films are presented in Figure 2. A clear difference was observed in the wetting behavior of the two groups: one group (5 and 10 vol%) has the microstructure of MWNTs embedded in a silicone matrix; the other (20 and 30 vol%) has a microstructure containing a large number of porous openings among entangled MWNTs with a thin silicone coating on the surfaces. The former group displayed smaller contact angles below 140° and larger sliding angles over 90°. On the contrary, the latter group showed larger contact angles and smaller sliding angles (<5°). The largest contact angle (and the smallest sliding angle) was observed on the 20 vol% MWNT–silicone composite film. The

best superhydrophobic state is known to be acquired in a micro–nano hierarchical structure, as is the case with lotus leaves. Although individual MWNTs can only result in a nanostructure, MWNT bundles can function as a micro–nanostructure, which is inevitable as one of the optimal superhydrophobic conditions. For CNT–polymer composite films, the distribution and order of CNT entanglement are important to embody optimal wetting characteristics. The composite with MWNT 20vol% is assumed to possess an ideal structure by distributing individual CNTs in the bundles at optimal locations. Nanopores in the composite coatings are assumed to help form the "Cassie state," too many porous areas could bring about degradation of the "Cassie structure", as shown in the 30 vol% MWNT–silicone specimen. Though nanopores could work as air pockets under water drop, water could infiltrate into large pores, which would turn Cassie state into Wenzel state. The wetting characteristics of the coatings on Al substrates generally agreed with those on Si substrates.

Frost growth on superhydrophobic MWNT–silicone coatings

Frost growth on superhydrophobic MWNT/–silicone composite coatings was observed in comparison to that on a bare Al substrate. The growth of frost on the 20 vol% MWNT–silicone coating was evaluated by holding the specimen inside a refrigerator at -30 °C for up to 650 min. Frost formation on the MWNT 20 vol.% MWNT–silicone composite (right-hand side) after being stored for 350 min storage at -30°C is presented with its counterpart on a bare Al substrate (left-hand side) in Figure 3(a). The specimen consisted of many Al pins, where half of them were coated with the MWNT–silicone composite and the other half were remained untreated. Contact angle and sliding angle of water on bare Al substrate were 88° and 90°, respectively. The average thicknesses of the frost grown on both surfaces are shown in Figure 3(b), where the growth rate of the frost on the superhydrophobic surface was about a half of that on the bare Al surface. Cao et al.[4] reported that superhydrophobic coatings with small particles (dimensions < 50 nm) showed long freezing delay. In this study, frost formation occurred rather irregularly on the MWNT–silicone composites, as shown in Figure 3(a), unlike the continuous formation and growth on the overall surface of a silica–polymer composite.

The radius of the critical nucleus (r_c) can be estimated with equation (1), as shown below:

$$r_c = -2\gamma\rho/\Delta G, \quad (1)$$

where γ is the water-–ice interfacial tension (0.034 $J \cdot m^{-2}$), ρ is the water molar volume (1.8×10^{-5} $m^3 \cdot mol^{-1}$), and ΔG is the free energy of formation ($\Delta G = -C_p \cdot T[\ln(T/T_m) + T_m/T - 1]$). In this study, the heat capacity of water (C_p) is 75.3 $J \cdot mol^{-1} \cdot K^{-1}$ at -30 °C. With these material properties, a value of 9.5 nm was obtained for r_c, which was smaller than the value of 21.6 nm obtained at -20°C.[4] Extensive supercooling of water resulted in a smaller radius of critical nucleation. Ice formation did not occur on the silica–polymer composites with silica particle diameters of 20 and 50 nm, since the filler size was comparable to the diameter of the critical nucleus (~43 nm). For the MWNT–silicone composite, the MWNT diameter (~12 nm) was smaller than the diameter of the critical nucleus (19 nm). From the calculation, nucleation of frost occurs more easily on MWNT bundle than on individual MWNT. Number of CNT and specific shape constituting MWNT bundles may affect the non-uniform frost formation. The experimental results imply that a small filler size could result in freezing delay, which is consistent with previous reports.[4-10]

In addition to nucleation aspect described above, recent research dealt with the effect of frost growth process on freezing delay and non-uniformity of frost formation. J. B. Boreyko et al. reported that superhydrophobic condenser could minimize frost formation by continuously removing subcooled condensate and limiting success of interdrop ice bridge formation.[23] In their observation, majority of drop diameters were 5~20μm on the hydrophobic film, while they were 40~60μm on the superhydrophobic film at -10℃. Their research was conducted with water drops larger than 5μm. Therefore, it is assumed that initial stage of freezing process could be more related with nucleation effect and the later part with growth process.

Stress relaxation behavior of superhydrophobic MWNT–silicone coatings

To evaluate the variations in stress of the MWNT–silicone composites, the stress values were measured as a function of temperature using the laser curvature method. The temperature of the system was varied from -100 °C to 80 °C to cover the entire range of temperatures for the thermal cycling test discussed in the next section. The stress values of the composite coatings, extracted from the measurements, are presented in Figure 4. Since the MWNT–silicone coatings had relatively large variations in thickness compared to thin films prepared by physical (or chemical) vapor deposition, the data are presented with a relatively large scatter. The overall change in stress over the temperature range was approximately 600 KPa for the film with 5 vol% MWNT, and the value increased as the MWNT content increased, with an exception of the 30 vol% MWNT–silicone specimen.

The elastic moduli and CTEs of the MWNT–silicone composites were evaluated by assuming an isotropic model with a random distribution of MWNTs in the silicone matrix (see Figure S1 in Supporting Information).[24-31] Here, theoretical calculations of the elastic modulus, CTE, and thermal stress were conducted with the assumption that all the composite coatings, regardless of MWNT content, had completely filled microstructures without any pores.[31] The elastic moduli of the composite coatings increased as the MWNT content increased, while the reverse trend was true of the values of CTE. Rapid change in the elastic modulus was observed when the MWNT content was over 80%, while that of CTE was found when the MWNT content was below 10%. The rate of change in CTE in the composite materials depended significantly on the aspect ratio of the MWNT filler. As the aspect ratio of the MWNT filler increased, most of the changes in CTE value were observed at the edge of the left-hand side of the graph (low filler content). For example, at a MWNT content of 5 vol%, the CTE value was 13.9 in this study (aspect ratio: 1000), while it increased to 60.7 and 176.4 when the aspect ratio was reduced to 100 and 10, respectively, showing that the majority of CTE changes occurred when the MWNT content was below 5 vol% if the aspect ratio was sufficiently large, as is the case with this study. Guo et al.[29] also reported that CTE of their PAN–40 wt%

SWNT composite was 34 times lower than that for pure PAN, which was close to that of SWNT. Similarly, the value of CTE of the 40 wt% MWNT–silicone composite in this study was 37 times lower than that of pure silicone.

The theoretical thermal stress increased rapidly as the MWNT content of the composite increased, as shown in Figure 5. The relative ratios of the thermal stresses increased to almost four times as the MWNT content was increased from 5 vol% to 30 vol%. The calculation was conducted with the stress value of the 5% MWNT–silicone composite film set as the reference point (see Table S2). Also, stress relaxation induced from plastic deformation of the silicone matrix or defects in the composite films was ignored for simplicity. The trend of stress change as a function of MWNT content suggests that the elastic modulus was more important than CTE for stress evolution in the composite films.

However, the experimental measurements showed that the superhydrophobic structures in the 20 and 30 vol%-MWNT specimens, which contained numerous pores, could accommodate high levels of thermal stress, thereby resulting in much lower stress value than those of the closed structures of the 5 and 10 vol%-MWNT specimens without any pores. The stress relaxation was estimated by comparing the theoretical thermal stresses (assuming closed structures) with experimentally measured stresses presented in Figure 4. Experimental stress variations with respect to temperature change were extracted from the slopes of the measured values and are listed in Table S2. By comparing the experimental values to the theoretical stress ratios, it is clear that a large amount of stress relaxation resulted from the nanoporous structures of the superhydrophobic films (inset of Figure 5). The stress relaxation reached 48 and 84% of the reference point for the 20 and 30%-MWNT specimens, respectively.

Reliability of MWNT–silicone coatings under thermal cycling condition

Anti-frost coatings can be applied to power lines and buildings to prevent ice accumulation and collapse of the constructions. They can also be used for surface coatings of heat exchangers inside air conditioners or refrigerators where temperatures rise and fall repeatedly. Thermal cycling tests were conducted to investigate the mechanical reliability of MWNT–silicone composite coatings on Al substrates. For the composite film containing 10 vol% MWNT, a 20 vol% MWNT–silicone film was chosen for the test since its superhydrophobic properties were superior to those of the coating containing 30 vol% MWNT even though the latter was better for stress relaxation. The changes in the contact and sliding angles of the composite coatings on Al substrates are presented in Figure 6 as functions of cycling number. The composite film containing 20 vol% MWNT endured 4000 cycles without significant change in the wetting angle. On the other hand, the wettability was degraded only after 400 cycles for the composite film containing 10 vol% MWNT, where the contact angle was 134° at first but dropped below 120° as the cycling number increased. Meanwhile, the sliding angle of the former film remained below 5°, while that of the latter film remained unchanged at 90° until the end of the test.

To investigate the surface morphologies and their correlation with wetting characteristics, cross-sectional SEM micrographs of the composite coatings were examined after 1000 cycles. The surface morphology of the coating containing 20 vol% MWNT, presented in Figure 7a,b, showed no serious change in comparison to its initial form in Figure 1c, which was consistent with the wetting behavior shown in the experiment. Its superhydrophobic surface consisted of a network of MWNT bundles and contained a large number of nanopores. On the other hand, after 1000 cycles, many cracks were formed on the surface of the composite coating containing 10 vol% MWNT, as shown in Figure 7c,d. The cracks formed inevitably since the films could not relax their accumulated thermal stresses, as discussed in detail in the previous section. Since CTE of silicone (310 ppm·°C^{-1}) is much larger than that of MWNT (7 ppm·°C^{-1}), the large expansion and shrinkage of the silicone matrix compared to the MWNT fillers resulted in MWNTs pulling out in a direction normal to the cracks, as shown in Figure 7d. The experimental results suggest that material design is of great importance to gain better reliability of superhydrophobic coatings, which can be achieved by combining superior wetting characteristics and reliable mechanical properties. Reliable mechanical design can be attained by selecting materials with the proper physical parameters (elastic modulus, CTE, aspect ratio of the filler and so on) for the composite film and substrate. Under thermal cycling condition, thermomechanical reliability can be enhanced by choosing a composite film and a substrate with similar values of CTE, although it appears impractical to select a hard filler and a soft matrix with similar CTE values.

Conclusions

Frost growth and mechanical reliability of superhydrophobic MWNT–silicone composite coatings were investigated under thermal cycling condition. The closed structure with MWNTs embedded in a silicone matrix did not maintain superhydrophobic characteristics and revealed mechanical vulnerability (film cracking with MWNTs pulling out) after repeated thermal cycling. On the other hand, the open structure with a large number of nanopores among MWNT bundles showed good superhydrophobic characteristics and mechanical sustainability, with a large amount of stress relaxation. From the experimental results, it is concluded that nanopores in superhydrophobic coatings, constituting air pockets in a "Cassie structure," are of great importance not only for wetting characteristics but also for superior reliability induced by stress relaxation. Although a more open structure can help relax more stress evolving from CTE mismatch, the composition of a superhydrophobic coating should be carefully selected to optimize its wetting characteristics and mechanical reliability. Following this rule, we designed a superhydrophobic MWNT–silicone composite with high reliability that endured over 4000 thermal cycles by controlling the microstructure of the composite.

At an experimental temperature of -30 °C, the critical radius for ice nucleation was calculated to be 9.5 nm. Although ice could not nucleate on the surface of individual MWNTs at this temperature, it could nucleate on MWNT bundles. Therefore, the distribution and order of entanglement of nanofillers in superhydrophobic composites are critical for freezing delay. To slow down frost thickening, the size and shape of nanofillers should be carefully chosen for superhydrophobic composites.

Acknowledgements

The acknowledgements come at the end of an article after the conclusions and before the notes and references.

References

1 H. Saito, K. Takai, G. Hamauchi, *Surf. Coat. Int.* 1997, **80**, 168.
2 P. Tourkine, M. L. Merrer, D. Quéré, *Langmuir* 2009, **25**, 7214
3 M. He, J. X. Wang, H. L. Li, X. L. Jin, J. J. Wang, B. Q. Liu, Y. L. Song, *Soft Matter* 2010, **6**, 2396.
4 L. L. Cao, A. K. Jones, V. K. Sikka, J. Z. Wu, D. Gao, *Langmuir* 2009, **25**, 12444.
5 F. C. Wang, C. R. Li, Y. Z. Lv, F. C. Lv, Y. F. Du, *Cold Regions Sci. Tech.* 2010, **62**, 29.
6 Z. Liu, Y. Gou, J. Wang, S. Cheng, *Int. J. Heat Mass Tran.* 2008, **51**, 5975.
7 L. Mishchenko, B. Hatton, V. Bahadur, J. A. Taylor, T. Krupenkin, J. Aizenberg, *ACS Nano* 2010, **4**, 7699.
8 S. A. Kulinich, M. Farzaneh, *Appl. Surf. Sci.* 2009, **255**, 8153.
9 Qiaolan Zhang, Min He, Xiping Zeng, Kaiyong Li, Dapeng Cui, Jing Chen, Jianjun Wang, Yanlin Song, Lei Jianga, *Soft Matter* 2012, **8**, 8285.
10 S. Jung, M. Dorrestijn, D. Raps, A. Das, C. M. Megaridis, D. Poulikakos, *Langmuir* 2011, **27**, 3059.
11 K. S. Lau, J. Bico, K. B. Teo, M. Chhowalla, G. A. Amaratunga, W. I. Milne, G. H. Mckinley, K. K. Gleason, *Nano Lett.* 2003, **3**, 1701.
12 D. Xu, H. Liu, L. Yang, Z. Wang, *Carbon* 2006, **44**, 3226.
13 L. Ci, S. M. Manikoth, X. Li, R. Vajtai, P. M. Ajayan, *Adv. Mater.* 2007, **19**, 3300.
14 J. Zou, H. Chen, A. Chunder, Y. Yu, Q. Huo, L. Zhai, *Adv. Mater.* 2008, **20**, 3337.
15 J. T. Han, S. Y. Kim, J. S. Woo, G. W. Lee, *Adv. Mater.* 2008, **20**, 3724.
16 J. Yang, Z. Zhang, X. Men, X. Xu, *Appl. Surf. Sci.* 2009, **255**, 9244.
17 D. Nyström, P. Antoni, S. Holdcroft, A. Hult, E. M. Jonsson, G. Vamvounis, *Soft Matter* 2012, **8**, 5753.
18 K. Wang, N. X. Hu, G. Xu, Y. Qi, E. M. Jonsson, G. Vamvounis, *Carbon* 2011, **49**, 1769.
19 L. Y. Meng, S. J. Park, *J. Coll. Inter. Sci.* 2010, **342**, 559.
20 T. Wu, Y. Pan, L. Li, *Coll. Surf. A* 2011, **384**, 47.
21 A. B. D. Cassie, S. Baxter, *Trans. Faraday Soc.* 1944, **40**, 5464.
22 A. Lafuma, D. Quéré, *Nature Mater.* 2003, **2**, 457.
23 J. B. Boreyko, C. P. Collier, *ACS Nano.* 2013, **7**, 1618.
24 D. Qian, E. C. Dickey, R. Andrews, T. Rantell, *Appl. Phys. Lett.* 2000, **76**, 2868.
25 K. M. Liew, X. Q. He, C. H. Wong, *Acta Mater.* 2004, **52**, 2521.
26 F. Y. Wu, H. M. Cheng, *J. Phys. D: Appl. Phys.* 2005, **38**, 4302.
27 J. P. Lu, *Phys. Rev. Lett.* 1997, **79**, 1297.
28 *Information about Dow Corning brand Silicone encapsulants*. Form No. 10-898I-01.
29 H. Guo, T. V. Sreekumar, T. Liu, M. Minus, S. Kumar, *Polymer* 2005, **46**, 3001.
30 P. K. Mallick, *Composites Engineering Handbook*, Marcel Dekker, New York, USA 1997.
31 D. S. Gardner, P. A. Flinn, *IEEE Trans. Electron Devices* 1988, **35**, 2160.

Journal Name RSCPublishing

ARTICLE

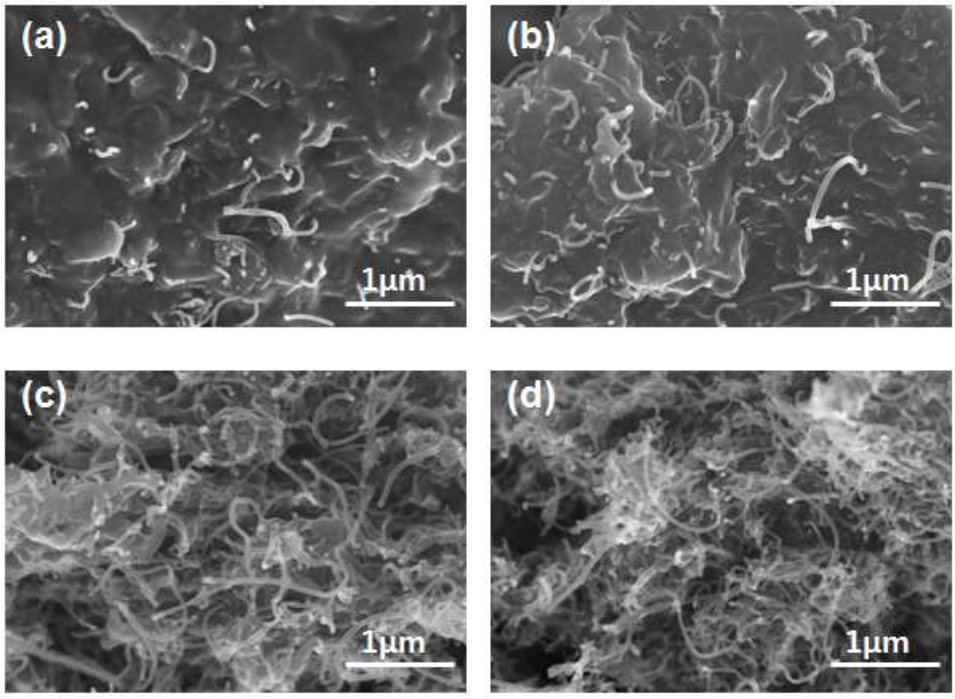

Figure 1. SEM micrographs of MWNT–silicone composite coatings on Al substrates as a function of MWNT content: (a) 5 vol%; (b) 10 vol%; (c) 20 vol%; (d) 30 vol%. The composite coatings containing 20 and 30 vol% MWNT showed open structures with numerous nanopores among the MWNTs, while closed structures were observed in the coatings containing 5 and10 vol% MWNT.

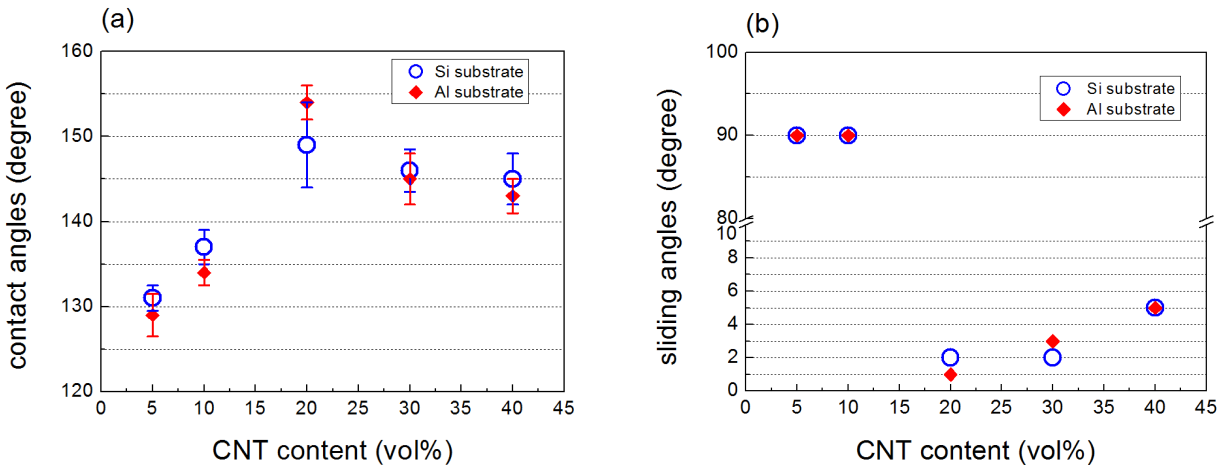

Figure 2. Measured (a) contact angles and (b) sliding angles of the MWNT–silicone composite coatings deposited on Al and Si substrates as a function of MWNT content. The coatings containing 5 and 10 vol% MWNT showed poor wetting characteristics, while those containing 20 and 30 vol% MWNT exhibited superior wetting properties.

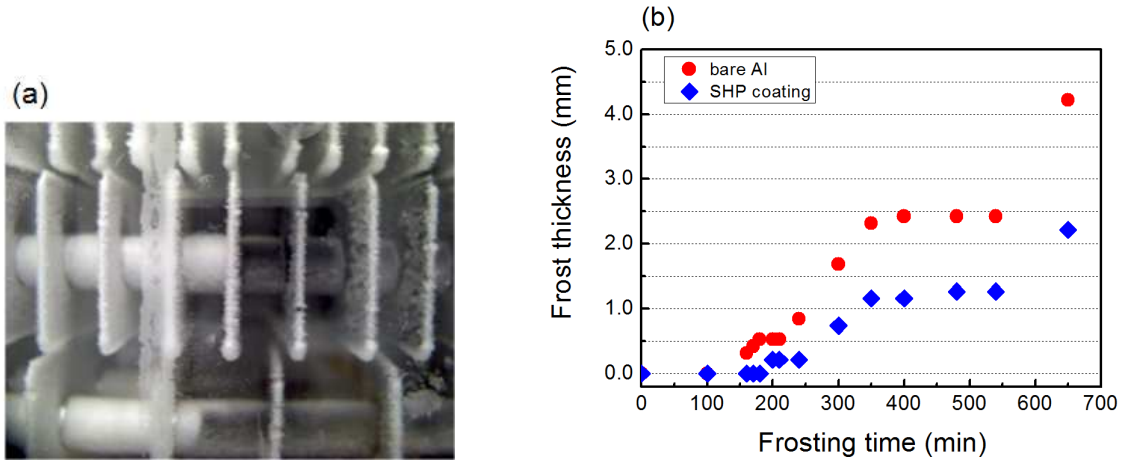

Figure 3. (a) Observation of frost growth on the composite coating containing 20 vol% MWNT at -30 °C (right-hand side), in comparison to that on bare Al substrate (left-hand side). The specimen consisted of many Al pins, where half of them were coated with the MWNT–silicone composite and the other half remained untreated. (b) Comparison of frost growth rate on the superhydrophobic coating (20 vol% MWNT) with that on a bare Al substrate.

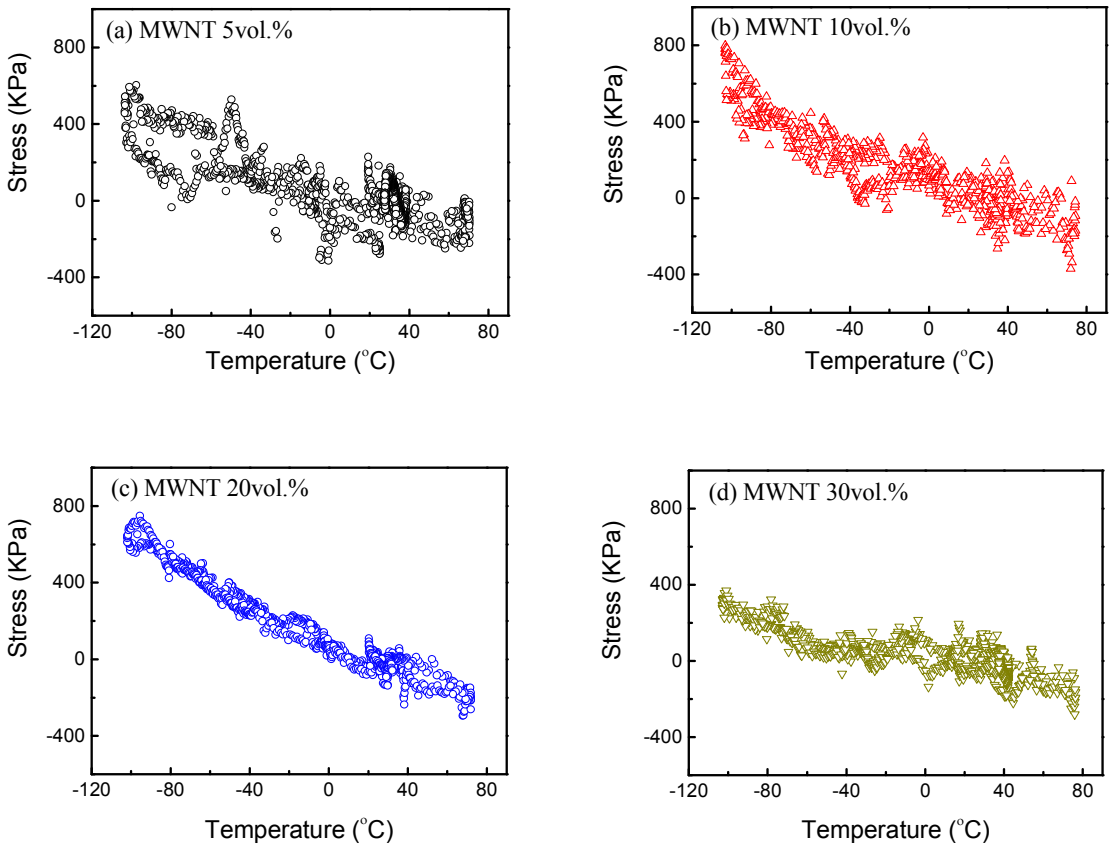

Figure 4. Measured stresses of the MWNT–silicone composite coatings on Si (100) substrates. The temperature of the system was varied from -100 °C to 80 °C to cover the entire temperature range of thermal cycling test presented in Figure 6. The variations in stress as functions of temperature were extracted from the slopes of the curves presented in the graphs.

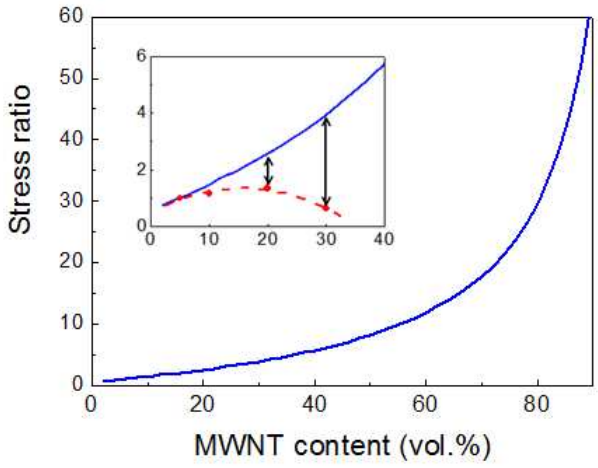

Figure 5. The relative ratios of thermal stresses evolved in the MWNT–silicone composite coatings. The solid line represents the theoretical calculated values, while dashed line represents the values extracted from experimental measurements presented in Figure 4. The stress value of the composite containing 5 vol% MWNT was set as the reference point: σ(5 vol% MWNT) = 1.

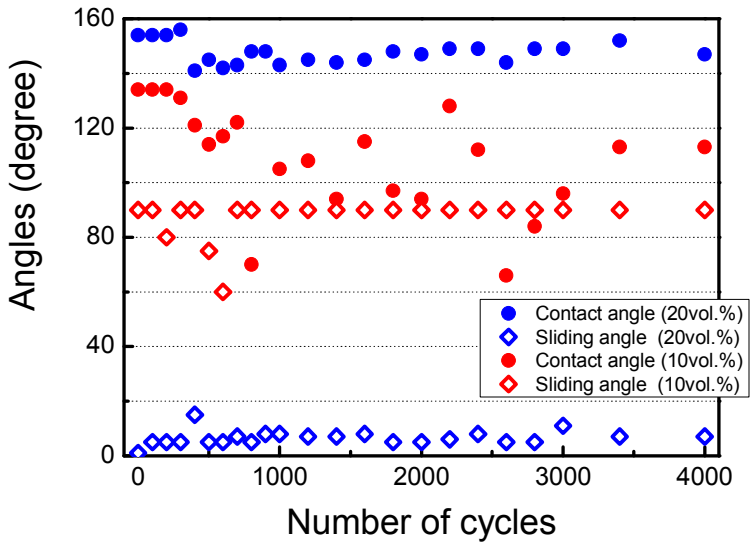

Figure 6. Changes in water contact and sliding angles on the MWNT–silicone composite coatings deposited on Al substrates as functions of thermal cycling number. The composite coating containing 20 vol% MWNT passed 4000 cycles without serious change in contact and sliding angles. On the other hand, the wetting properties were degraded only after 400 cycles for the composite containing 10 vol% MWNT.

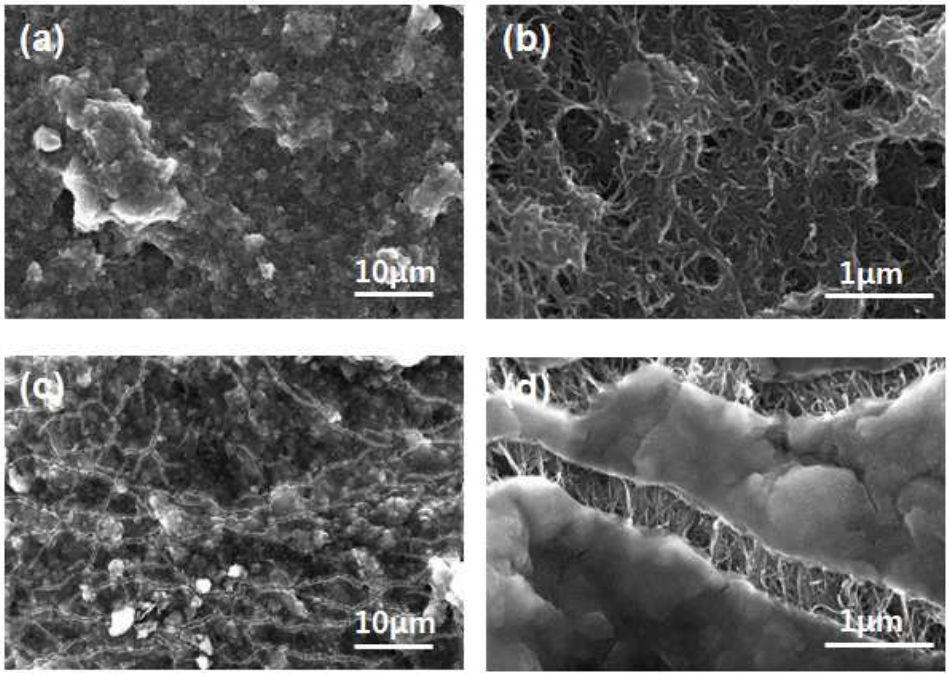

Figure 7. SEM micrographs showing morphologies of the MWNT–silicone composite coatings deposited on Al substrates after 1000 cycles of the thermal cycling test. The composite coating containing 20 vol% MWNT is presented in (a) and (b). The composite coating containing 10 vol% MWNT is presented in (c) and (d), where a great number of cracks were generated from the large thermal stress during the thermal cycling test.